A functional role for *Tsix* transcription in blocking *Xist* RNA accumulation but not in X-chromosome choice

Nicholas Stavropoulos, Naifung Lu, and Jeannie T. Lee*

Howard Hughes Medical Institute, Department of Molecular Biology, Massachusetts General Hospital, and Department of Genetics, Harvard Medical School, Boston, MA 02114

Edited by Stanley M. Gartler, University of Washington, Seattle, WA, and approved June 8, 2001 (received for review May 16, 2001)

In female mammals, up-regulation of *Xist* triggers X-chromosome inactivation in cis. Up-regulation is inhibited by sequences 3′ to *Xist* contained within the antisense locus, *Tsix*. Inhibition could depend on transcription of *Tsix* and/or on DNA elements therein. Here we test the role of *Tsix* transcription by augmenting the duration and strength of *Tsix* expression. We find that *Tsix* hypertranscription is sufficient to block *Xist* RNA accumulation in a cis-limited manner. We propose that *Tsix* transcription is necessary to restrict *Xist* activity on the future active X and, conversely, that *Tsix* repression is required for *Xist* RNA accumulation on the future inactive X. We also find that *Tsix* hypertranscription does not affect X-chromosome choice. Thus, choice is mediated by elements within *Tsix* that are independent of promoter activity.

X-inactivation, the transcriptional silencing of a single X chromosome during female embryogenesis, ensures equal dosage of X-linked genes in male (XY) and female (XX) mammals (ref. 1; reviewed in ref. 2). During the process of X-inactivation, a counting mechanism determines X-chromosome number, a choice mechanism randomly selects one active and one inactive X chromosome, and a silencing mechanism operates on the chosen inactive X to shut down expression of nearly all genes in cis. Numerous genetic studies have established the noncoding X-linked gene, *Xist*, as the trigger for silencing (3–9). At the onset of cellular differentiation, *Xist* RNA accumulates on all but one randomly selected X in each cell, an event sufficient for X-chromosome silencing (9) and "coating" of the inactive X by *Xist* transcripts (3, 10).

How *Xist* RNA accumulation is blocked on the future active X remains poorly understood. With the use of mouse embryonic stem (ES) cells to model X-inactivation *in vitro*, recent genetic studies have implicated the sequences 3′ to *Xist* in X-chromosome choice and in regulating *Xist* accumulation in cis (11, 12). In both studies, female cells heterozygous for 3′ deletions maintain two active X's before differentiation and properly undergo inactivation of a single X upon cell differentiation. However, the mutated X is almost always chosen for *Xist* accumulation, resulting in severe skewing of X-inactivation in differentiated populations. Thus, elements removed by these deletions function in cis to regulate X-chromosome choice and to prevent *Xist* RNA accumulation.

The 3.7-kb region common to both deletions spans a CpG-rich domain and the putative promoter of *Tsix*, a gene antisense to *Xist* (13). *Tsix* initiates 15 kb downstream of the *Xist* 3′ terminus and produces a noncoding transcript extending across the entire *Xist* locus. The expression pattern of *Tsix* is consistent with a role in regulating *Xist* (13). All active X chromosomes express *Tsix* before differentiation, a time when *Xist* expression is low. *Tsix* expression is extinguished before *Xist* RNA accumulation on the future inactive X. On the future active X, *Tsix* expression persists until *Xist* expression is silenced. Thus, the loss of *Tsix* expression is closely associated with an increased steady-state level of *Xist* transcripts in cis. Although the consequences of deleting *Tsix* demonstrate its involvement in X-chromosome choice and in *Xist* repression, the molecular basis of these two activities has not been established. These activities may depend on DNA sequences within the 3.7-kb region deleted by the $Tsix^{\Delta CpG}$ knockout (12). Alternatively, they may depend on *Tsix* transcription or on the antisense transcript itself.

In mammals, many antisense genes have been described, especially within domains subject to imprinting (reviewed in ref. 14). In the murine *Igf2r* locus, a CpG island associated with an oppositely imprinted antisense RNA is required for imprinting of *Igf2r* (15). In the Prader–Willi/Angelman locus, the maternally expressed *UBE3A* gene is associated with paternally expressed antisense transcripts (16). As in the case of *Xist* and *Tsix*, the functional significance of these antisense transcripts has remained unclear. Specifically, do antisense genes work through DNA elements associated with them, or is their expression necessary for the inhibitory effect on sense genes?

Here we address whether *Tsix* transcription plays a role in *Xist* regulation. We augment and extend *Tsix* expression by inserting a constitutive promoter into one *Tsix* allele in XX ES cells. This gain of function is sufficient to block *Xist* accumulation and X-inactivation in cis but does not affect X-chromosome choice. Because this allele removes no sequences, we suggest that altered X-chromosome choice in previous *Tsix* deletions is caused by the loss of DNA elements that regulate choice independently of antisense transcription. Thus, these results support separate functional roles for *Tsix* transcription in antagonizing *Xist* accumulation and for DNA elements in regulating X-chromosome choice.

Materials and Methods

Cell Lines and Culture Conditions. To generate the targeting vector, a hybrid human *EF-1α*/HTLV 5′ long terminal repeat promoter (bp 374-1563 of GenBank J04617 fused to bp 373–647 of GenBank J02029) that confers constitutive expression in murine cell lines (F. Randow and B. Seed, personal communication) was coupled to a 1.9-kb *Bam*HI–*Sal*I *Tsix* fragment and placed in the *Xho*I site of pLNTK (17). The adjacent 5.8-kb *Bam*HI fragment of *Tsix* was placed in the *Sal*I site of pLNTK. *Tsix* sequence was of *129* origin. Linearized targeting vector was electroporated into 16.7 (12), G418- and ganciclovir-resistant colonies were selected (targeting frequency 6/141), and the *Neo* cassette was excised, all as performed elsewhere (12). ES and embryoid body (EB) cell culture conditions have been described (12). For analysis of

This paper was submitted directly (Track II) to the PNAS office.

Abbreviations: ES, embryonic stem; EBs, embryoid bodies; RT-PCR, reverse transcription–PCR; FISH, fluorescence *in situ* hybridization.

See commentary on page 10025.

*To whom reprint requests should be addressed at: Department of Molecular Biology, Massachusetts General Hospital and Department of Genetics, Harvard Medical School, Boston, MA 02114. E-mail: lee@frodo.mgh.harvard.edu.

The publication costs of this article were defrayed in part by page charge payment. This article must therefore be hereby marked "*advertisement*" in accordance with 18 U.S.C. §1734 solely to indicate this fact.

differentiation, EBs were allowed to adhere to plates on day 4 to enable cellular outgrowth.

Reverse Transcription–PCR (RT-PCR). For allele-specific RT-PCR, RNA was isolated with Trizol (GIBCO/BRL), DNase treated (1 unit/5 μg of RNA), and reverse transcribed at 37°C with Moloney murine leukemia virus RT (GIBCO/BRL) and 200 ng of random primer, or at 50°C with Superscript II (GIBCO/BRL) and 3 pmol of strand-specific primer. Single-nucleotide polymorphisms 2.3 kb and 25.3 kb downstream from the *Tsix* initiation site yield additional *Mnl*I and *Scr*FI sites respectively, on the *Mus musculus castaneus* X chromosome. Transcripts containing these polymorphisms were amplified with the use of flanking primers in RT-PCR (30 cycles: 94°C 45 s, 55°C 45 s, 72°C, 1 min). RT-PCR product was diluted 12.5-fold into fresh PCR mixture and cycled once to minimize heteroduplex DNA, digested with *Mnl*I or *Scr*FI to liberate polymorphic *M. m. castaneus* and *129* fragments, fractionated on agarose gels, blotted, and detected by hybridization to designated ^{32}P-end-labeled primers. Phosphorimaging (Molecular Dynamics) was used to obtain quantitative measures of relative allelic amounts, as PCR products differ by only a single base substitution and are amplified and detected with primers identical in *129* and *M. m. castaneus*. Primers A-I shown in Fig. 2*A* are, respectively, NS30 5′-CCCTGCTTGCTCAACTCTACG-3′, NS31 5′-TTAGCCCGCATCTCACCCAC-3′, NS18 5′-GGTAACAATTTTCCCGCCATGTG-3′, NS22 5′-TGCGATAACTTTCTTTGAGAAGCCTTGGAAGTTGAGACCT-3′, NS19 5′-GGAAATAAACGGAACGCAGTACC-3′, NS33 5′-CAGAGTAGCGAGGACTTGAAGAG-3′, NS67 5′-CCAGAGTCTGATGTAACGGAGG-3′, NS60 5′-CCCGCTGCTGAGTGTTTGATATG-3′, and NS66 5′-GCTGGTTCGTCTATCTTGTGGG-3′. *Rrm2* primers are as described (18). For quantitative RT-PCR, *Xist* and *Rpo2–1* were coamplified for 22 cycles with primers NS33, NS66, Rpo2–1a 5′-GGACTAATGGATCCACGGCAG-3′, and Rpo2–1b 5′-GGTCATAGACATGCGTAAGCCG-3′. *Oct3/4* was coamplified with *Rrm2* for 20 cycles with Rrm2 primers, Oct3a 5′-GGCGTTCTCTTTGGAAAGGTGTTC-3′ and Oct3b 5′-CTCGAACCACATCCTTCTCT-3′. Both reactions were within exponential amplification ranges as determined by pilot experiments. NS66, Oct3a, Rpo2–1a, and Rrm2a were ^{32}P-end-labeled, and RT-PCR products were separated on acrylamide gels.

Fluorescence *in Situ* Hybridization (FISH). Double-stranded probes for *EF-1α*, *Tsix*, and *Xist* were labeled with tetramethylrhodamine-5-dUTP or fluorescein-12-dUTP and used in RNA-FISH as described (12). Single-stranded *Tsix* and *Xist* riboprobe cocktails were generated by *in vitro* transcription with fluorescein-12-UTP and digoxigenin-11-UTP, respectively, and visualized with rhodamine-conjugated anti-digoxigenin antibody (Roche Molecular Biochemicals). *Mecp2* probes were as described (12). *Xist* probe cocktails were complementary to exons 1 and 7.

Cell Death Analysis. Sedimented day 2 and 4 EBs were dispersed by trypsinization and stained with trypan blue. Live and dead cells were scored on a hemacytometer, and the percentage of dead cells was calculated. Alternatively, whole cultures (including supernatant and EBs) were counted. The results were similar in the two cases.

Results

Insertion of the *EF-1α* Promoter Provides High-Level and Persistent *Tsix* Expression. We inserted the constitutive human *EF-1α* promoter upstream of the major *Tsix* transcription start sites (*Tsix*$^{EF\text{-}1\alpha}$ allele, Fig. 1*A*) by homologously targeting one allele in XX ES cells. The 16.7 ES line carries polymorphic X chromosomes derived from *M. m. castaneus* (X^{cas}) and *129* (X^{129}) strains

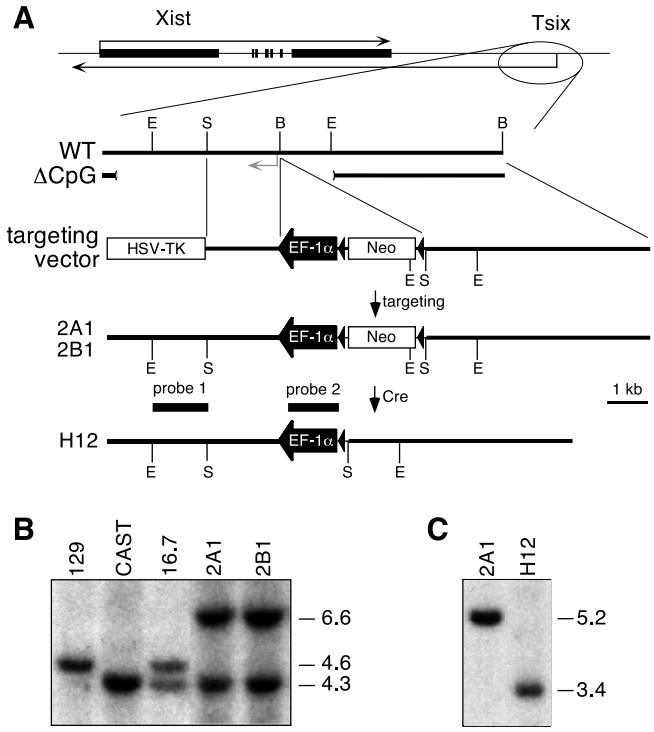

Fig. 1. Construction of the *Tsix*$^{EF\text{-}1\alpha}$ allele. (*A*) Map of the *Xist*/*Tsix* locus and targeting scheme. Gray arrow, *Tsix* transcription initiation site (ref. 13; RNase protection; N.S., unpublished results). Dark triangles, loxP sites. ΔCpG indicates the region removed by the *Tsix* knockout (12). B, *Bam*HI; E, *Eco*RI; S, *Sal*I. (*B*) Southern blot analysis of controls and two representative mutant lines, 2A1 and 2B1. Genomic DNA was digested with *Eco*RI and hybridized to probe 1. *129* and *M. m. castaneus* *Eco*RI fragments are polymorphic (19). (*C*) Southern blot analysis of parental 2A1 and *Neo*-excised subclone H12. H12 was derived from 2A1 by transient expression of Cre recombinase. Genomic DNA was digested with *Sal*I and hybridized to probe 2.

(12). As determined by an *Eco*RI polymorphism (19) flanking the targeted region, all insertion events occurred on X^{129} (Fig. 1*B*; data not shown). Mutant lines containing (lines 2A1, 2B1; Fig. 1*B*) and lacking (line H12; Fig. 1*C*) the *PGK-Neo* selection marker were analyzed in parallel. All lines behaved similarly.

In the undifferentiated state, mutant and wild-type cells grew indistinguishably. RT-PCR analysis indicated that transcription was correctly initiated within the *EF-1α* promoter and extended into *Tsix* (Fig. 2 *A* and *B*). An allele-specific RT-PCR assay able to distinguish X^{cas} and X^{129} *Tsix* transcripts revealed that *Tsix*$^{EF\text{-}1\alpha}$ increased the steady-state level of *Tsix* RNA in cis (Fig. 2 *C* and *D*). In 16.7 cells, 35% of total *Tsix* RNA was derived from X^{129}. In contrast, 60% was of X^{129} origin in mutant cells. Assuming that transcription from X^{cas} was similar in 16.7 and mutant cells, this difference indicated that *Tsix*$^{EF\text{-}1\alpha}$ increased steady-state RNA levels by approximately 3-fold in cis. This elevation was observed at 5′ and 3′ positions within *Tsix* (Fig. 2 *A*, *C*, and *D*), suggesting that transcripts initiated from the *EF-1α* promoter proceeded through at least 25 kb of *Tsix* and covered most of the *Xist* locus. RNA FISH analysis also showed that *Tsix*$^{EF\text{-}1\alpha}$ was overexpressed. Like wild-type cells, all (>95%) undifferentiated mutant cells showed two nuclear *Tsix* RNA foci but differed in that the *Tsix*$^{EF\text{-}1\alpha}$ signal was larger and more intense than that of the untargeted allele (91% with $X^{129} > X^{cas}$, $n = 277$; Fig. 2*E*). Together, these data showed that insertion of the *EF-1α* promoter increased the strength of *Tsix* expression in cis.

Tsix expression is asynchronously down-regulated in female cells during differentiation, with down-regulation occurring first

GENETICS

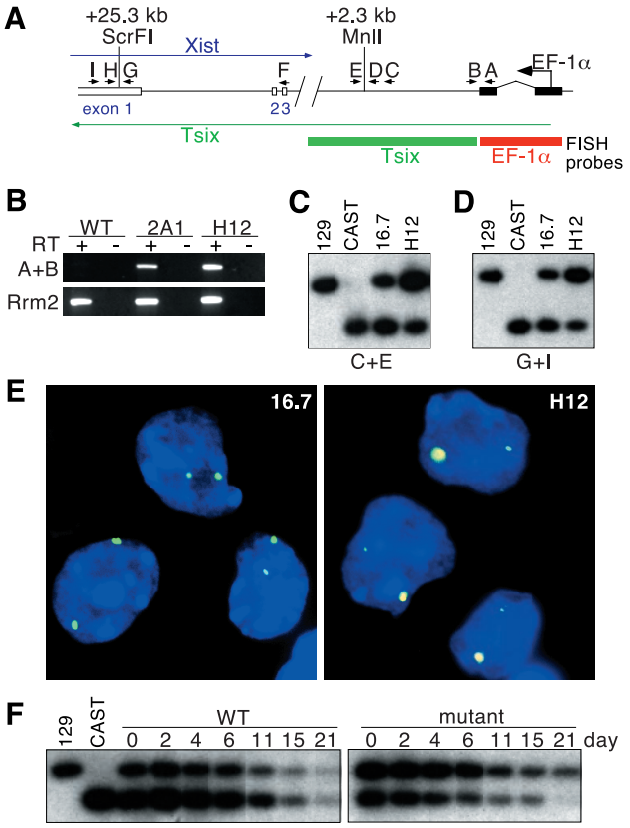

Fig. 2. The *EF-1α* promoter confers high-level, persistent *Tsix* expression. (*A*) Map of the $Tsix^{EF\text{-}1\alpha}$ locus. *Xist* exons 1, 2, and 3 are depicted at the left. Locations of primers A–I and distances of *M. m. castaneus* restriction polymorphisms from the *Tsix* initiation site are denoted. (*B*) Transcriptional fusion of the EF-1α leader to $Tsix^{EF\text{-}1\alpha}$ transcripts. *Rrm2* (ribonucleotide reductase M2), positive control. (*C*) *Tsix* 5′ allele-specific RT-PCR. cDNA was generated with primer E and amplified with primers C and E. Polymorphic *129* and *M. m. castaneus* MnlI fragments were detected by hybridization to primer D. No amplification was observed in RT samples (data not shown). (*D*) *Tsix* 3′ allele-specific RT-PCR. cDNA was generated with primer I and amplified with primers G and I. Polymorphic *Scr*FI fragments were detected by hybridization to primer H. (*E*) RNA-FISH of undifferentiated wild-type (16.7) and mutant (H12) cells, with double-stranded *EF-1α* (red) and *Tsix* (green) probes shown in *A*. (*F*) Allele-specific RT-PCR analysis of *Tsix* in wild-type (16.7) and mutant (2B1) cells on different days of differentiation. Random-primed cDNA was amplified with primers C and E, and *Mnl*I fragments were detected with D.

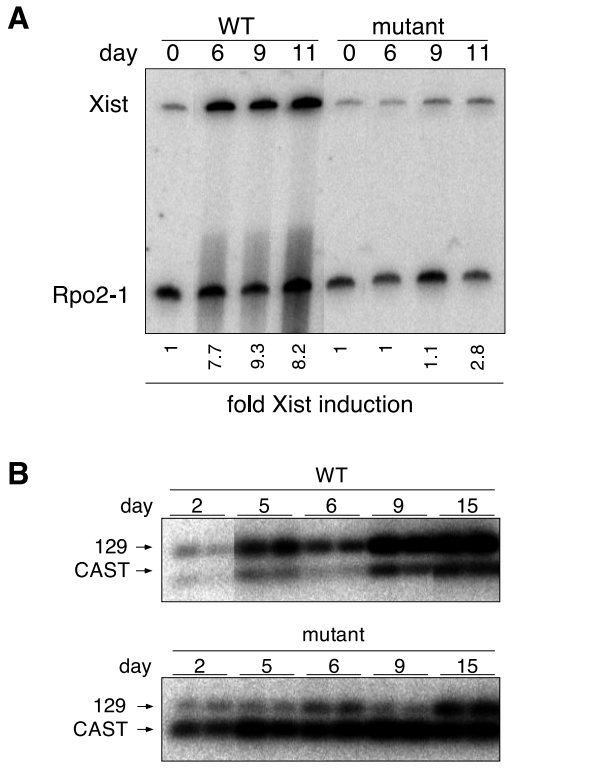

Fig. 3. Effects of $Tsix^{EF\text{-}1\alpha}$ on *Xist* expression under differentiation conditions. (*A*) Quantitative RT-PCR for *Xist* expression in wild-type (16.7) and mutant (H12) cells placed under differentiation conditions for the number of days shown. *Xist* levels were normalized to *Rpo2–1* levels; fold *Xist* induction reflects the change from day 0. (*B*) Allele-specific *Xist* RT-PCR of wild-type (16.7) and mutant (2B1) cells. Amplification was carried out with primers F and H (spanning *Xist* introns, as shown in Fig. 2*A*) and polymorphic *Scr*FI fragments detected with G.

on the future inactive X and subsequently on the future active X after *Xist* expression is silenced (13). This finding has raised the possibility that persistence of *Tsix* expression on one X is critical for maintaining its active state. To determine whether insertion of the *EF-1α* promoter extended the duration of *Tsix* expression from X^{129}, we cultured ES cells in the absence of LIF for 2 to 21 days to induce differentiation into EBs (20), a state that normally induces down-regulation of *Tsix*. As in undifferentiated cells, we found that, whereas wild-type 16.7 cells expressed more *Tsix* RNA from X^{cas}, mutant cells consistently displayed more $Tsix^{EF\text{-}1\alpha}$ RNA from X^{129} throughout differentiation (Fig. 2*F*). Moreover, the fraction of total *Tsix* RNA originating from $Tsix^{EF\text{-}1\alpha}$ increased progressively during differentiation, suggesting not only that $Tsix^{EF\text{-}1\alpha}$ conferred stronger expression, but that expression persisted beyond that of the unmodified *Tsix* allele on X^{cas}.

To test this idea further, we performed FISH on mutant cells that were placed under differentiation conditions for 6 to 13 days. On day 6, *Tsix* expression from the mutant locus was detectable in nearly all cells. In cells with monoallelic *Tsix* signals, two-color FISH with *EF-1α* and *Tsix* probes indicated that antisense transcripts nearly always originated from the $Tsix^{EF\text{-}1\alpha}$ allele (99%, $n = 108$). On day 13, *Tsix* RNA was still present in >60% of mutant cells, whereas it was seen in <5% of wild-type cells. In mutant cells, *Tsix* signals originated only from $Tsix^{EF\text{-}1\alpha}$ (data not shown). Notably, monoallelic *Tsix* expression was not detected from X^{cas} on either day 6 or day 13 cultures. These findings provided further evidence that the *EF-1α* promoter conferred persistent expression under differentiation conditions.

$Tsix^{EF\text{-}1\alpha}$ Suppresses *Xist* Accumulation in cis. We examined the effects of $Tsix^{EF\text{-}1\alpha}$ on *Xist* expression when mutant cells were placed under differentiation conditions to induce X-inactivation. As demonstrated by quantitative RT-PCR, *Xist* expression in both mutant and wild-type cells was low before the onset of X-inactivation (Fig. 3*A*). This observation indicated that *Tsix* overexpression did not affect steady-state *Xist* levels before initiation of X-inactivation. Upon placement in differentiation conditions, wild-type cells showed an 8.2-fold induction of *Xist* relative to RNA polymerase II large subunit (*Rpo2–1*). In contrast, mutant cells exhibited only a 2.8-fold induction (Fig. 3*A*). This reduced level of *Xist* induction might reflect compromised *Xist* induction in all mutant cells or, alternatively, compromised *Xist* induction in a subset of the population. In the latter case, the overall level as measured by RT-PCR would be the weighed average of *Xist* expression across different cell populations.

We next used allele-specific RT-PCR to examine *Xist* induc-

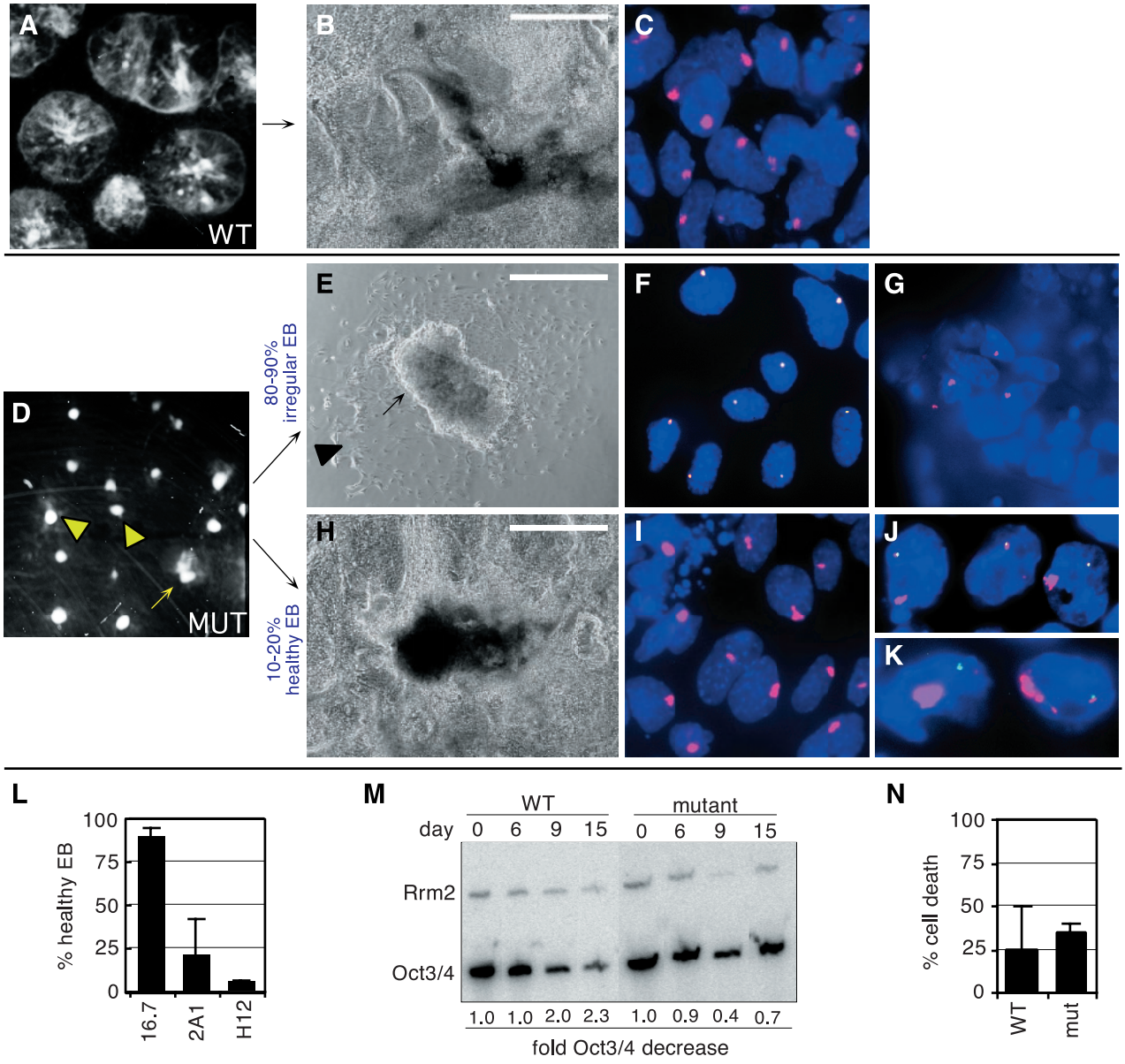

Fig. 4. Differentiation conditions yield two types of mutant cells. (*A*) Dark-field micrograph of control EBs from 16.7 cells on day 9. (*B*) A phase-contrast micrograph of day 15 16.7 EBs shows well-differentiated structures. (Scale bar = 100 μm.) (*C*) RNA FISH with single-stranded *Xist* probes (red) of day 9 16.7 EB cells. (*D*) Dark-field micrograph of typical mutant EB cultures on day 9 (H12). Triangles: small, irregular EBs; the EB on the left contains one sector of differentiation. Arrow: medium-sized, healthy EB with many sectors of well-differentiated cells. (*E*) Phase-contrast micrograph of a typical poorly differentiated day 15 mutant EB (H12). The arrow points to a poorly differentiated ES-like cluster. The triangle points to a partially differentiated outgrowth. (*F*) RNA FISH of cells in a representative small irregular EB, with EF-1α (green) and double-stranded *Tsix* probes (red). Experiments with *Tsix*-specific probes yielded identical results (data not shown). *EF-1*α signals identify X^{129}. (*G*) RNA FISH of cells from a representative irregular EB, with single-stranded *Xist* probes (red), on day 9 mutant cells (H12). (*H*) A representative healthy mutant EB (H12). (*I*) RNA FISH of a representative healthy mutant EB on day 9, with single-stranded *Xist* probes (red). (*J*) RNA FISH of mutant (H12) cells on day 4, with double-stranded probes to *EF-1*α (green) and *Xist* (red). (*K*) RNA FISH of day 4 mutant (H12) cells, with double-stranded *Xist* (red) and *Mecp2* probes (green). (*L*) Percentage of EBs showing healthy growth in 16.7 (wild type), 2A1, and H12 (mutant). (*M*) Quantitative RT-PCR for *Oct3/4* expression in wild-type (16.7) and mutant (H12) cells placed under differentiation conditions for the number of days shown. *Oct3/4* levels were normalized to *Rrm2* levels; the fold *Oct3/4* decrease reflects the change from day 0. (*N*) Cell death analysis of wild-type (16.7) and mutant (H12) EBs. Results indicate the average of day 2 and day 4 samples. Data represent the average of at least four independent experiments. Error bars indicate one standard deviation.

tion from wild-type and mutant X chromosomes. In the parental 16.7 line, *Xist* from X^{129} accounted for 85% of total *Xist* RNA (Fig. 3*B*). This skewing reflects biased X-chromosome choice found in *129/castaneus* hybrid mice and has been attributed to effects of the X-controlling element (Xce) modifier (21). X^{cas} carries a strong Xce^{c} relative to X^{129} (Xce^{a}) and is more likely to remain active (22). Analysis of mutant cultures revealed a striking reversal of the *129/castaneus Xist* ratio, with X^{129} providing only 10–15% of total *Xist* RNA (Fig. 3*B*). Therefore, despite an intrinsic bias for expressing the *129* allele in the parental cell line, *Xist* accumulation in mutant cells was chiefly from *M. m. castaneus* from days 2 to 9. In late day cultures, the expression of the *129* allele increased somewhat, a finding we believe to stem from growing numbers of poorly differentiated cells specific to late-day mutant cultures (see below; these ES-like cells apparently expressed low levels of *Xist* from both X chromosomes).

The results of these RT-PCR experiments suggested that

reduced total *Xist* expression in mutant cultures resulted from the failure to up-regulate *Xist* from the mutant X^{129} chromosome. To address this possibility further, we analyzed single cells with RNA FISH, as described below.

X-Chromosome Choice: Two Distinct Cell Fates in Mutant Cultures. To perform single-cell analysis, ES cells were placed under differentiation conditions for 9–15 days to obtain EB outgrowths for RNA FISH. In this assay, small groups of ES cells aggregate and grow into EBs for 4 days in suspension culture. On day 4, the cells are allowed to adhere to the culture dish, whereupon differentiating cells migrate from the EB core as a monolayer of mixed cell types (20). Wild-type cultures consistently yielded large, well-differentiated EBs (Fig. 4*A*) with typical structures such as beating hearts and tubular networks (Fig. 4*B*). High-level *Xist* expression was present in >90% of wild-type cells ($n > 2{,}000$; Fig. 4*C*). Analysis of mutant cultures revealed a dramatically different phenotype, with differentiation conditions yielding two distinct EB types.

The more prevalent type of EB was strikingly small and accounted for 80–90% of the total (Fig. 4 *D* and *L*). These EBs showed irregular growth, with some sectors of the EB growing more robustly than others (Fig. 4*D*, triangles). The small irregular EBs lacked beating hearts, tube networks, and other obvious differentiated structures. Interestingly, they had large central cell clusters that resembled undifferentiated ES colonies, in that the clusters had smooth borders and bright, refractile centers (Fig. 4*E*, arrow). These clusters were often surrounded by cells that appeared to be partially differentiated in morphology (Fig. 4*E*, triangle). In contrast to cells of wild-type EBs, cells in these EBs continued to express *Tsix* from the mutant X chromosome (Fig. 4*F*; 85–90% with expression, $n > 2{,}000$) and lacked *Xist* RNA accumulation (85–90% of cells without *Xist* signals, $n > 2{,}000$; Fig. 4*G*). Thus, small irregular EBs were dominated by cells that failed to undergo X-inactivation. As prior studies have linked cell differentiation and X-inactivation (23, 24), we surmise that the poor overall differentiation in these EBs resulted from the inability of most cells to undergo X-inactivation.

The second type of EB had an intermediate size and accounted for 10–20% of the total (Fig. 4*D*, arrow, and Fig. 4*L*). As in wild-type EBs, differentiated structures, including beating hearts and tubular networks, were regularly observed (Fig. 4*H*). Similarly, high-level *Xist* expression was seen in ≈90% of differentiating outgrowths (Fig. 4*I*, $n > 2{,}000$). $Tsix^{EF\text{-}1\alpha}$ RNA signals could still be detected in 50–60% of cells within healthy EBs and, importantly, did not colocalize with *Xist* RNA accumulation. The remaining 40% of cells could not be scored because *EF-1α* RNA signals were not visible, and attempts at *EF-1α* DNA FISH were unsuccessful because of the small size (1.4 kb) of the *EF-1α* probe. To circumvent this problem, we examined earlier day cultures where $Tsix^{EF\text{-}1\alpha}$ RNA was expressed in >95% of all cells. On day 4 (Fig. 4*J*), two-color RNA FISH revealed that 95% ($n = 127$) of *EF-1α* signals were spatially distinct from high-level *Xist* signals. Thus, *Xist* accumulation occurred almost exclusively from X^{cas}. This pattern of nonrandom X-inactivation was consistent with the results of allele-specific RT-PCR (Fig. 3*B*) and suggested that transcription from $Tsix^{EF\text{-}1\alpha}$ is sufficient to block *Xist* RNA accumulation in cis. On X^{cas}, accumulation of *Xist* RNA led to silencing of *Mecp2* (87%, $n = 281$; Fig. 4*K*), indicating that the silencing step of X-inactivation was not affected by the $Tsix^{EF\text{-}1\alpha}$ allele expressed in trans. Unlike in the small irregular EBs, the abundance of cells that underwent successful, albeit skewed, X-inactivation in the healthy EBs probably permitted the formation of well-differentiated structures.

The poor overall differentiation of mutant cultures was consistent with higher levels of the ES-specific marker *Oct3/4* (25) (Fig. 4*M*). Because failure to compensate for X-linked gene dosage is toxic to development (7, 26), the *in vitro* fate of cells that failed to up-regulate *Xist* was of some interest. Cell death was not elevated in mutant cultures (Fig. 4*N*). Instead, there was an increase in cell number within the poorly differentiated ES-like clusters during late-day culture (Fig. 4*E* and data not shown). This result suggested that cells that failed to up-regulate *Xist* were able to remain viable in a poorly differentiated state.

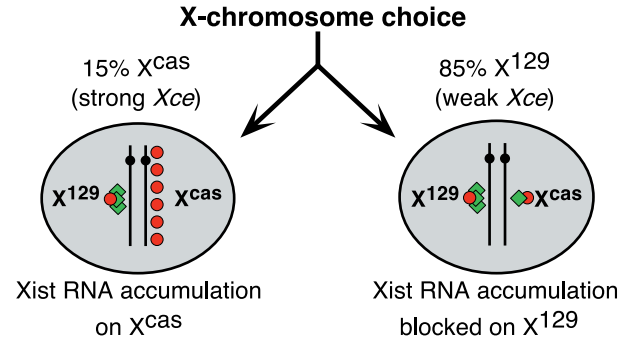

Fig. 5. Model: X-chromosome choice is not disrupted by the $Tsix^{EF\text{-}1\alpha}$ allele. *Xist* RNA, red circles; *Tsix* RNA, green diamonds. See text for details.

Thus, placing the mutant cells in differentiation conditions yielded two cell fates. In one, *Xist* could not be up-regulated and cells remained poorly differentiated in appearance. In the other, *Xist* RNA could accumulate to high levels, but did so primarily from X^{cas}. These cells showed healthy differentiation. In both classes of cells, expression from $Tsix^{EF\text{-}1\alpha}$ was observed. We propose that the two fates reflected an epigenetic decision made before the initiation of *Xist* expression. Specifically, we suggest that the decision regarding X-chromosome choice was not affected by $Tsix^{EF\text{-}1\alpha}$. In this model (Fig. 5), mutant cells would retain the ability to count and randomly choose one active and one inactive X. In the parental cell line (16.7), X^{129} was inactivated 85% of the time. We suggest that, likewise, the mutant cell lines chose X^{129} for inactivation 85% of the time, but that high-level and persistent antisense transcription from $Tsix^{EF\text{-}1\alpha}$ precluded accumulation of *Xist* RNA in cis. In this model, mutant cells would choose X^{cas} for inactivation 15% of the time. Indeed, we found that an average of 10–20% of cells from all mutant EBs showed a high level of *Xist* expression. The random distribution of *Xist*-expressing and -nonexpressing cells among different EB colonies would then determine the degree of differentiation within individual EBs and thereby determine whether they appeared irregular or healthy.

Although we favor this model, we also considered alternative explanations for the two cell fates. One possibility was that the *EF-1α* insertion affected X-chromosome counting and prevented X-inactivation as a result. This possible outcome appeared less likely to us, however, because 10–20% of the cells properly inactivated one X chromosome, with inactivation highly specific for X^{cas}. Another possibility was that the *EF-1α* insertion nonspecifically affected cell differentiation. This explanation was also not favored, because a reproducible subpopulation of mutant cells could differentiate and form healthy EBs. Furthermore, the extreme bias toward inactivating X^{cas} cannot be explained by a defect in cell differentiation alone. For these reasons, our data support the explanation that expression from $Tsix^{EF\text{-}1\alpha}$ provides a secondary block to *Xist* accumulation and X-inactivation without affecting X-chromosome choice.

Discussion

We have addressed the question of whether transcription plays a role in the inhibitory effect of *Tsix* on *Xist* by creating a gain of function in *Tsix* transcription. Insertion of the constitutive human *EF-1α* promoter enabled us to distinguish the effect of

transcription from that of specific DNA elements. Although the $Tsix^{EF\text{-}1\alpha}$ allele did not delete any sequence within *Tsix*, it is possible that the disruption of endogenous sequence by the *EF-1α* insertion could have contributed to the phenotype. We consider this outcome unlikely, however, given that a disruption would have more likely yielded a loss-of-function than a gain-of-function phenotype. Importantly, the $Tsix^{EF\text{-}1\alpha}$ allele produced a pattern of nonrandom inactivation that is the opposite of that in the $Tsix^{\Delta CpG}$ loss-of-function mutation, a mutation that led to nearly exclusive inactivation of the mutant X. In the gain-of-function mutant, we showed that augmentation of *Tsix* transcription was sufficient to block *Xist* accumulation on the mutant X chromosome. This result demonstrates that *Tsix* transcription is indeed functional.

Our results directly support the hypothesis that silencing of *Tsix* expression is a prerequisite for *Xist* up-regulation on the future inactive X. Consistent with this hypothesis, prior study showed that *Tsix* is repressed before or around the same time that *Xist* RNA accumulates in cis (13). Furthermore, *Xist* transgenes lacking the 5′ end of *Tsix* and therefore presumably lacking antisense expression are all permissive for high-level *Xist* expression (8, 9). We also suggest that, conversely, *Tsix* transcription on the future active X is necessary to maintain X-chromosome activity in female cells. Indeed, *Tsix* persists transiently on the presumptive active X even after *Xist* RNA has accumulated on the newly inactivated X (13). Inhibition of *Xist* may require either increased levels of *Tsix* expression or a mere prolongation of *Tsix* transcription. The means by which *Tsix* transcription inhibits *Xist* accumulation is not yet clear; the act of *Tsix* transcription could interfere with *Xist* accumulation indirectly, or, alternatively, inhibition could depend on the antisense RNA product.

Finally, our findings uncover a role for *Tsix* that is independent of transcription. The disruption of X-chromosome choice by $Tsix^{\Delta CpG}$, but not by $Tsix^{EF\text{-}1\alpha}$, implies that a DNA element within the 3.7 kb removed by $Tsix^{\Delta CpG}$ mediates the act of choice. Classic models of X-inactivation have postulated the existence of a "blocking factor," a trans-acting factor that mediates choice by binding to one X and preventing *Xist* from initiating chromosome-wide silencing (reviewed in ref. 27). It is therefore possible that the DNA element implied by our results acts as a binding site for the putative blocking factor. Binding of the factor could elevate or prolong *Tsix* transcription and thereby block *Xist* up-regulation. In this model, *Tsix* transcription is epistatic to choice and is itself sufficient to prevent the initiation of long-range silencing of the X chromosome.

The abundance of noncoding and antisense genes within imprinted regions has suggested that they are critical to the mechanism of allelic exclusion. The present work establishes the importance of their transcription. Our findings contrast with the report that *H19* and its transcription are dispensable for imprinting *Igf2* (28, 29). Antisense transcripts have also been reported for *Igf2* (30), but their significance remains unknown at this time. The antisense gene, *Air*, within the *Igf2r* locus contains necessary information for *Igf2r* imprinting (15), but whether its transcription is important also remains unclear. Within the Prader–Willi/Angelman syndrome region, many imprinted genes have associated antisense transcription or are themselves genes for noncoding RNAs (reviewed in ref. 31). Given the diverse nature of these transcripts and their associated imprinted domains, it is likely that many mechanisms are involved in the regulation of imprinting. Antisense transcription may be only one of many mechanisms.

We thank B. Seed and F. Randow for the EF-1α promoter; S. Dymecki for Cre reagents; J. Urbach and D. Wilson for discussion of heteroduplex formation; G. Lazar for aid with photography; and W. Chao, D. Cohen, J. Conaty, K. Huynh, C. Kaplan, R. Spencer, F. Winston, and T. Wu for critical reading of the manuscript and discussions. This work was supported by Howard Hughes Medical Institute Predoctoral and Ryan fellowships (to N.S.) and grants from Hoechst, the March of Dimes (Basil O'Connor Scholarship), and the National Institutes of Health (to J.T.L.). J.T.L. is also a Pew Scholar and an assistant investigator for the Howard Hughes Medical Institute.

1. Lyon, M. F. (1961) *Nature (London)* **190,** 372–373.
2. Heard, E., Clerc, P. & Avner, P. (1997) *Annu. Rev. Genet.* **31,** 571–610.
3. Brown, C. J., Hendrich, B. D., Rupert, J. L., Lafreniere, R. G., Xing, Y., Lawrence, J. & Willard, H. F. (1992) *Cell* **71,** 527–542.
4. Brockdorff, N., Ashworth, A., Kay, G. F., McCabe, V. M., Norris, D. P., Cooper, P. J., Swift, S. & Rastan, S. (1992) *Cell* **71,** 515–526.
5. Penny, G. D., Kay, G. F., Sheardown, S. A., Rastan, S. & Brockdorff, N. (1996) *Nature (London)* **379,** 131–137.
6. Lee, J. T., Strauss, W. M., Dausman, J. A. & Jaenisch, R. (1996) *Cell* **86,** 83–94.
7. Marahrens, Y., Panning, B., Dausman, J., Strauss, W. & Jaenisch, R. (1997) *Genes Dev.* **11,** 156–166.
8. Herzing, L. B., Romer, J. T., Horn, J. M. & Ashworth, A. (1997) *Nature (London)* **386,** 272–275.
9. Wutz, A. & Jaenisch, R. (2000) *Mol. Cell* **5,** 695–705.
10. Clemson, C. M., McNeil, J. A., Willard, H. F. & Lawrence, J. B. (1996) *J. Cell Biol.* **132,** 259–275.
11. Clerc, P. & Avner, P. (1998) *Nat. Genet.* **19,** 249–253.
12. Lee, J. T. & Lu, N. (1999) *Cell* **99,** 47–57.
13. Lee, J. T., Davidow, L. S. & Warshawsky, D. (1999) *Nat. Genet.* **21,** 400–404.
14. Tilghman, S. M. (1999) *Cell* **96,** 185–193.
15. Wutz, A., Smrzka, O. W., Schweifer, N., Schellander, K., Wagner, E. F. & Barlow, D. P. (1997) *Nature (London)* **389,** 745–749.
16. Rougeulle, C., Cardoso, C., Fontes, M., Colleaux, L. & Lalande, M. (1998) *Nat. Genet.* **19,** 15–16.
17. Gorman, J. R., van der Stoep, N., Monroe, R., Cogne, M., Davidson, L. & Alt, F. W. (1996) *Immunity* **5,** 241–252.
18. Lee, J. T. & Jaenisch, R. (1997) *Nature (London)* **386,** 275–279.
19. Debrand, E., Chureau, C., Arnaud, D., Avner, P. & Heard, E. (1999) *Mol. Cell. Biol.* **19,** 8513–8525.
20. Martin, G. R. & Evans, M. J. (1975) *Proc. Natl. Acad. Sci. USA* **72,** 1441–1445.
21. Cattanach, B. M. & Isaacson, J. H. (1967) *Genetics* **57,** 331–346.
22. Cattanach, B. M. & Rasberry, C. (1994) *Mouse Genome* **92,** 114.
23. Monk, M. & Harper, M. I. (1979) *Nature (London)* **281,** 311–313.
24. Martin, G. R., Epstein, C. J., Travis, B., Tucker, G., Yatziv, S., Martin, D. W., Jr., Clift, S. & Cohen, S. (1978) *Nature (London)* **271,** 329–333.
25. Okamoto, K., Okazawa, H., Okuda, A., Sakai, M., Muramatsu, M. & Hamada, H. (1990) *Cell* **60,** 461–472.
26. Takagi, N. & Abe, K. (1990) *Development (Cambridge, U.K.)* **109,** 189–201.
27. Lyon, M. F. (1996) *Nature (London)* **379,** 116–117.
28. Jones, B. K., Levorse, J. M. & Tilghman, S. M. (1998) *Genes Dev.* **12,** 2200–2207.
29. Schmidt, J. V., Levorse, J. M. & Tilghman, S. M. (1999) *Proc. Natl. Acad. Sci. USA* **96,** 9733–9738.
30. Moore, T., Constancia, M., Zubair, M., Bailleul, B., Feil, R., Sasaki, H. & Reik, W. (1997) *Proc. Natl. Acad. Sci. USA* **94,** 12509–12514.
31. Mann, M. R. W. & Bartolomei, M. S. (1999) *Hum. Mol. Genet.* **8,** 1867–1873.